

# MAGMATIC AND POST-MAGMATIC SIGNIFICANCE OF CHROMITITE AND ASSOCIATED PLATINUM-GROUP MINERALS (PGM) IN THE EASTERN KHOY OPHIOLITIC COMPLEX (NW IRAN)

Amir M. Azimzadeh\*, Federica Zaccarini\*,✉, Mohsen Moayyed\*\*, Giorgio Garuti\*, Oskar A.R. Thalhammer\*, Ibrahim Uysal\*\*\* and Mirsaleh Mirmohammadi\*\*\*\*

\* Department of Applied Geosciences and Geophysics, University of Leoben, Austria.

\*\* Department of Earth Sciences, University of Tabriz, Iran.

\*\*\* Department of Geology, Karadeniz Technical University, Trabzon, Turkey.

\*\*\*\* School of Mining Engineering, University College of Science, Tehran University, Iran.

✉ Corresponding author: e-mail: federica.zaccarini@unileoben.ac.at

**Keywords:** Chromitites, ophiolite, platinum-group minerals, platinum-group elements. Khoys, Iran.

## ABSTRACT

The Khoys ophiolites are one of the largest Iranian ophiolitic complexes and are characterized by a very complicate geology, consisting of several ophiolites with different ages and geodynamic settings of formation. Few small lenticular and irregular bodies of podiform and schlieren type chromitites have been recognized in the Khoys ophiolites, occurring in the serpentinized mantle peridotites. They have massive and nodular textures.

According to their chromite composition, the Khoys chromitites can be classified as Al-rich and fall clearly in the field of podiform chromitites. The magmatic chromite composition of the podiform chromitites of the Khoys ophiolites suggests that they crystallized from a MORB type melt in an extensional regime. The Khoys chromitites were altered during ocean floor metamorphisms and no magmatic silicates were preserved. The composition of chlorite occurring in the silicate matrix or in contact with chromite has been used as a geothermometer. The estimated temperatures possibly reflect the effects of low-grade metamorphism.

The Khoys chromitites have very low total platinum group elements (PGE) concentration with a predominance of Os + Ir + Ru over Rh + Pt + Pd. Consistently with the geochemical data, they contain few platinum group minerals (PGM) of Ru, Ir and Os. Laurite is the most common PGM along with a minor Ir-Cu sulfide, possibly cuproiridsite, osmium and erlichmanite. Most of the PGM are magmatic in origin. They crystallized in a narrow range of temperature, around 1000°C, at relatively low sulfur fugacity and in the absence of fluids. This observation is consistent with formation of the chromitites in a mid-oceanic ridge (MOR) rather than in a supra-subduction zone (SSZ).

## INTRODUCTION

Chromite is an early liquidus phase crystallizing from mafic and ultramafic magmas over a wide range of conditions. It may occur either as an accessory mineral, mostly in peridotite, or as the major constituent of chromitite. Chromitites are economically relevant rocks, representing the only natural source for chromium recovery. They are conventionally grouped into two major types: (i) stratiform, associated with large mafic-ultramafic layered intrusions and (ii) podiform, mostly occurring in the mantle sequence of ophiolites.

Due to its chemical and physical properties, chromite is generally more resistant to alteration compared to the associated olivine and pyroxenes, which are usually altered into secondary paragenetic assemblages (i.e., serpentine, talc, chlorite and garnet). Even in the case of deep alteration, chromite may retain its primary magmatic composition at the core of partially altered grains, sometimes becoming the only petrogenetic indicator of the host rocks and of their geodynamic setting of formation (Irvine, 1965; 1967; Thayer, 1970). For this reason, an increasing amount of data concerning the primary composition of chromite and its geological interpretation has been collected in the decades (Dick and Bullen, 1984; Roeder, 1994; Stowe, 1994; Zhou and Robinson, 1997; Barnes and Roeder, 2001; Kamenestiy et al., 2001; Rollinson 2008).

Chromitites may host platinum group minerals (PGM) as accessory phases. Although the PGM occur as rare and tiny

grains (generally less than 10 microns in size) their chemical composition, paragenesis and texture have been used to model the mechanism of their precipitation under magmatic conditions (Zaccarini et al., 2011 and references therein).

This contribution focuses in particular on the magmatic significance of chromite composition and associated PGM and silicates in the podiform chromitites of the Khoys complex, located in the north-western part of Iran, never investigated before. The Khoys complex is characterized by a very complicate geology and according to Pessagno et al. (2005) it consists of at least two and possibly three ophiolitic units with different ages and geodynamic settings of formation. Therefore, the data presented in this contribution are used to try to define the geodynamic environment in which the Khoys chromitites were generated. Finally, taking into account that chromite exhibits, in some cases, compositional zoning as the result of alteration during serpentinization and metamorphism, we also discuss the influence of these post magmatic effects on the Khoys chromitite, using the data on texture and composition of the altered chromite and associated secondary minerals, mainly chlorite.

## GENERAL GEOLOGY OF THE IRANIAN OPHIOLITES AND DESCRIPTION OF THE ASSOCIATED CHROMITITES

The Tethyan ophiolite belt, Mesozoic in age, extending from Spain to the Himalayas is the longest ophiolite belt in

the world. According to recent literature data (Hoeck et al., 2002; Robertson, 2002), most of the Tethyan ophiolites cropping out from the Balkan Peninsula to Turkey formed in a suprasubduction zone (SSZ) rather than at the mid-oceanic ridge (MOR). Most of these SSZ ophiolites host chromite deposits, associated with dunite in the mantle peridotite that generally consists of partially to totally serpentinized harzburgite. Most of the Iranian ophiolites belong to the Middle East Tethyan belt that geographically links ophiolites of the Carpathian-Mediterranean sector to those located in the Himalayas.

The Iranian ophiolites play an important role in deciphering the geodynamic evolution of Middle Eastern Tethys, since they are characterized by different geochemical signatures varying from MOR-basalt, to island arc tholeiite (IAT) and SSZ derived melts (Hassanipak and Ghazi, 2000). Based on their geographical location, the Iranian ophiolites have been divided into four groups (Hassanipak and Ghazi, 2000 and references therein): (i) ophiolites of northern Iran along the Alborz Range, (ii) ophiolites of the Zagros Suture Zone, including the Neyriz and Kermanshah ophiolites, which appear to be coeval with the Oman (Samail) ophiolite, emplaced onto the Arabian continental margin, (iii) unfragmented ophiolites of the Makran accretionary prism which include the complexes of Band-e-Zeyarat/Dar Anar and Remeshk/Mokhtar Abad, and (iv) ophiolites and colored mélanges that mark the boundaries of the central Iranian microcontinent (CIM), including the Shahre-Babak, Nain, Baft, Sabzevar Tchehel Kureh ophiolites and Khoy (Fig. 1A).

According to the age of emplacement, Alavi (1991) divided the Iranian ophiolites into three main groups: (i) Proterozoic ophiolites that consist of isolated blocks, cropping out in the western limb of the Lut Block (central Iran), (ii) pre-Jurassic ophiolites mainly exposed in the Alborz Range in the north, and (iii) post-Jurassic ophiolites, the most abundant Iranian ophiolites.

More than 70 chromite occurrences have been documented in the Iranian ophiolites and 18 of them are currently mined (Yaghubpu and Hassannejad, 2006). Most of the Iranian chromitites occur in serpentinized mantle tectonites and have been classified as podiform chromitites. Few chromitites, exposed in southern Iran, show some similarity with stratiform type deposits. The Iranian chromitites are mainly concentrated in the following 4 areas (Malekghasemi and Somarin, 2005; Yaghubpur and Hassannejad, 2006):

1) The Sabzevar area (NE Iran). Here, chromitites form lenticular and fragmented layers associated with serpentinized dunite. Whole rock  $Cr_2O_3$  concentrations range from 30 to 45%.

2) The Esfandagheh and Fariab area (S-SE Iran). This is the most prominent mining area of Iran, since about 90% of Iranian chromite is extracted in this area. Chromite layers and lenses are associated with dunite, harzburgite and pyroxenite.

3) The Neyriz region (SE Iran). In this area, lenticular, massive, disseminated and nodular chromitites have been found. They occur mainly in harzburgite. Whole rock concentrations vary from 30 to 45%.

4) The Khoy region (NW Iran). Few chromitites have been recognized in this area, and currently there are no mining activities. Massive and nodular chromitites occur within serpentinized peridotite, forming lenticular and irregular bodies. No microprobe data are available regarding the chromite composition.

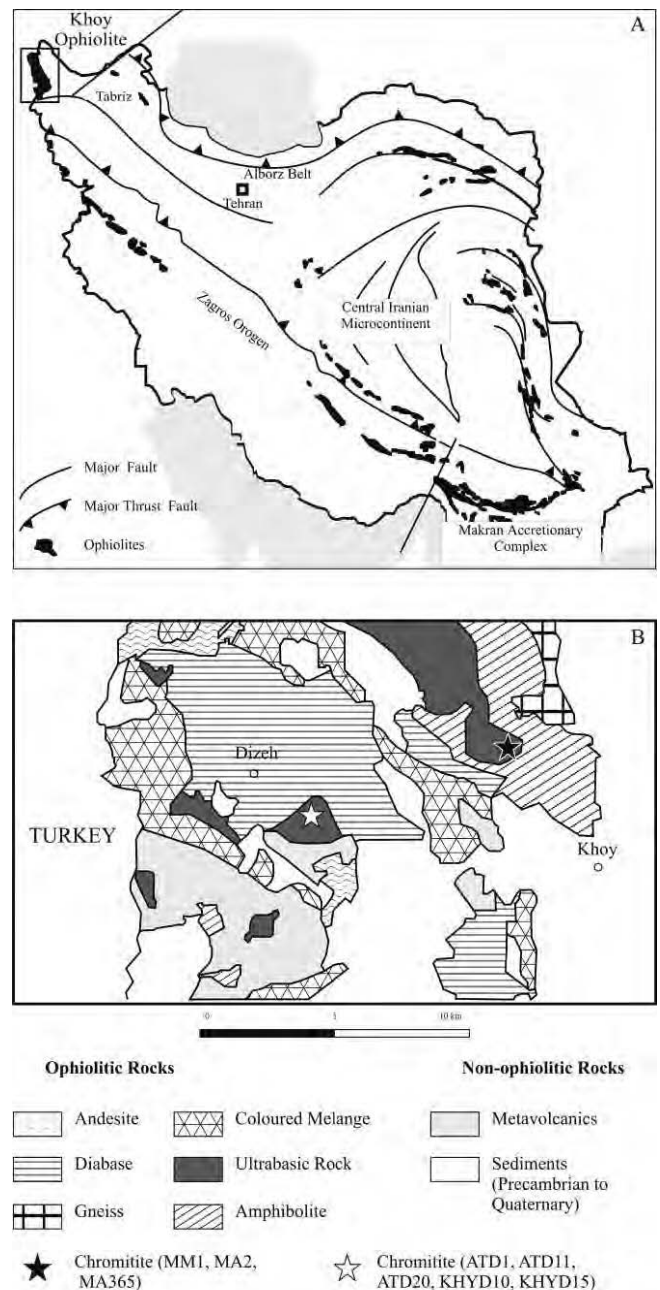


Fig. 1 - A. Simplified tectonic zones of Iran (after Alavi et al., 1997 and Ghazi et al., 2003). In black, the major ophiolite complexes. Location of the Khoy ophiolite is shown. B. Geological sketch map of the area of the Khoy ophiolite that hosts the investigated chromitites (simplified after Ghorashi and Arshadi, 1978; Hassanipak and Ghazi, 2000).

### GEOLOGY OF THE KHOY OPHIOLITE AND DESCRIPTION OF THE INVESTIGATED CHROMITITE

The Khoy ophiolite is one of the largest ophiolite complexes of Iran, covering an area of more than 700 km<sup>2</sup> (Fig. 1B). The Khoy ophiolite crops out in a strategic junction area, where the ophiolites of Iran connect with the Mediterranean and Turkish ophiolites (Pessagno et al., 2005). It is considered a fragment of the oceanic lithosphere formed in the Mesozoic Neo-Tethys (Hassanipak and Ghazi, 2000). According to these authors, it consists of a mantle sequence including dunite and harzburgite partially to totally serpen-

tinized, accompanied by minor chromitites. The mantle sequence is overlain by the following crustal rocks: cumulate gabbros, diorite, pillow and massive basalts, covered by a pelagic sedimentary sequence with umber and radiolarian chert.

Based on  $^{40}\text{K}/^{39}\text{Ar}$  geochronological data obtained on hornblende (Ghazi et al., 2003) and on the geochemical signature, at least two different complexes have been recognized in the Khoy area: the Western and the Eastern Khoy ophiolitic complexes, respectively (Khalatbari-Jafari et al., 2003; 2004; 2006). The first one is Late Cretaceous in age, whereas the latter is Early Jurassic to Early Cretaceous. The evolution of the Khoy complex is still matter of debate, owing to the fact that it consists of several dismembered and strongly tectonized blocks. Hassanipak and Ghazi (2000) proposed that the Khoy ophiolite originated along a MOR. Other authors suggested that the Eastern Khoy complex possibly formed in a slow-spreading back-arc basin, which was obducted over the tholeiitic and calcalkaline rocks of the adjacent island arc system during the Late Cretaceous (Monsef et al., 2010, and references therein).

Recently, Pessagno et al. (2005) recognized the following parts in the Khoy complex:

Area 1) Early Cretaceous amphibolites, constituting one ophiolite block, accompanied by Late Jurassic ophiolite remnants composed of tectonized ultramafic rocks and gabbros. The ultramafic rocks are in tectonic contact with the western portion of the amphibolites.

Area 2) Tectonic *mélange* composed of pelagic limestones, serpentinites and basalts with a possible OIB affinity. The *mélange* probably represents a subduction complex associated with an island arc (Khalatbari-Jafari et al., 2003).

Area 3) E-MORB and N-MORB pillow lavas, interbedded with Late Cretaceous pelagic limestones and siliceous mudstones, respectively.

Area 4) Late Cretaceous manganiferous cherts overlain disconformably by pyroclastic rocks.

The metamorphic evolution of the Khoy ophiolites is complex (Khalatbari-Jafari et al., 2003; Azizi et al., 2006). Some of the oldest ophiolite blocks, exposed in the eastern portion of the Khoy complex, experienced regional metamorphism up to amphibolite facies. Khalatbari-Jafari et al. (2003) recognized at least four metamorphic events which

occurred from Early Jurassic to Late Cretaceous. According to these authors, the metamorphosed Mesozoic eastern Khoy complex is composed of numerous ophiolite fragments that were piled up and tectonically stacked in a subduction accretion complex. Other younger ophiolite remnants, cropping out in the western Khoy complex, did not suffer regional metamorphism and are believed to have formed in a slow-spreading ridge setting (Khalatbari-Jafari et al., 2003).

The investigated chromitites were collected in two areas located respectively, about 5 km to the north-west and about 10 km west of the city of Khoy (Fig. 1B). The chromitites form several bodies, variable in size from a few up to ten meters, of podiform and schlieren type ores, associated with strongly serpentinized and tectonized peridotites (Fig. 2). These ultramafic rocks are those described in the Area 1 defined by Pessagno et al. (2005).

## METHODOLOGY

Oxides and silicates were analyzed by electron microprobe at the "Eugen F. Stumpfl Laboratory" of the Leoben University with a Superprobe Jeol JXA 8200. Back scattered electron (BSE) images were obtained using the same instrument. The primary composition of chromite was obtained in the unaltered cores of grains. In order to determine the compositional zoning, lines with point analyses each 15 microns apart, were carried out on selected chromite crystals. Analyses of chlorite were obtained on grains intergrown with altered chromite and from the matrix. The electron microprobe was operated in WDS mode, 15 kV accelerating voltage and 10 nA beam current. The analyses of Si, Mg, Al, Na, K, Ca, Ti, V, Cr, Mn, Fe, Ni and Zn were carried out using the  $K\alpha$  lines, and were calibrated on natural chromite, rhodhonite, clinopyroxene, albite, adular and ilmenite as reference materials, along with metallic V, Ni and Zn. The counting times for peak and backgrounds were 15 and 5 seconds, respectively. The amount of  $\text{Fe}^{3+}$  in chromite was calculated assuming the spinel stoichiometry  $\text{R}^{2+}\text{O R}^{3+}_2\text{O}_3$ . The detection limits of trace elements such as Si, T, Ni, Zn and V are the following (in ppm): 1600, 330, 438, 488 and 264, respectively. The analytical results are listed in Tables 1 and 2.

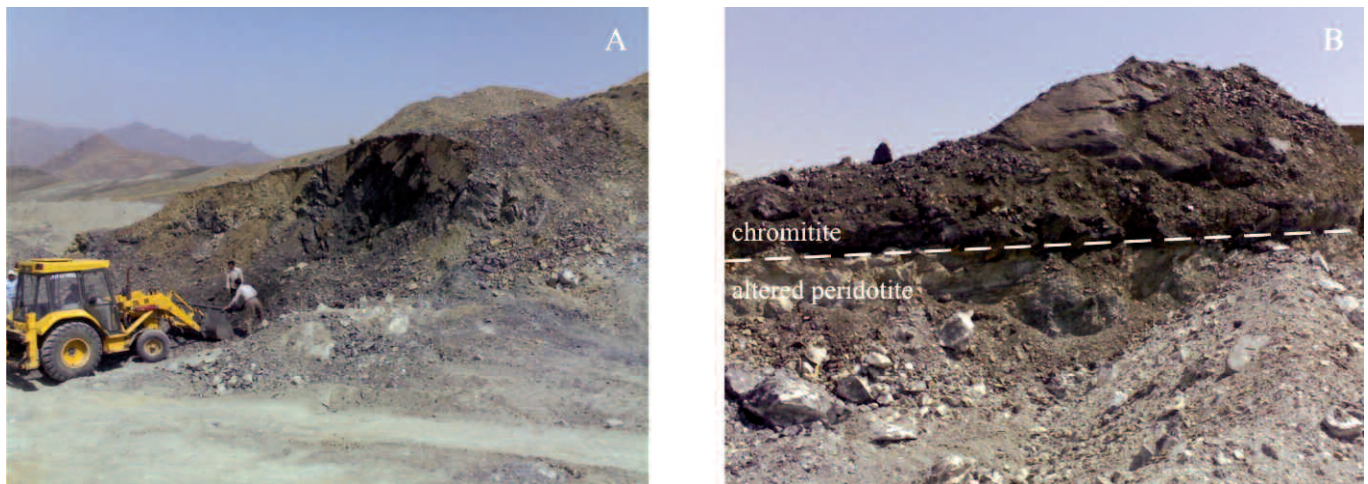


Fig. 2 - A. Field photographs of a small chromite mine in the Khoy ophiolite. B. Contact between chromitite and the strongly tectonized and altered peridotite host.

Table 1 - Average composition of the magmatic chromite of the Khoy chromitites.

Samples	MM1	MA2	MA365	ATD1	ATD11	ATD20
No. of analyses	50	49	50	15	15	15
SiO <sub>2</sub>	b.d.l	b.d.l	b.d.l	0.09	0.11	0.19
σ	-	-	-	0.11	0.13	0.15
TiO <sub>2</sub>	0.16	0.21	0.18	0.59	0.59	0.61
σ	0.01	0.02	0.01	0.02	0.02	0.03
Al <sub>2</sub> O <sub>3</sub>	26.12	32.29	31.19	21.32	21.73	20.95
σ	0.61	1.00	0.63	0.23	0.25	0.34
FeO*	14.63	14.37	14.35	15.89	17.12	16.62
σ	0.34	0.73	0.35	0.33	0.33	0.32
Fe <sub>2</sub> O <sub>3</sub> *	1.37	1.94	1.73	5.06	5.54	5.06
σ	0.33	0.53	0.33	0.47	0.33	0.61
MgO	13.45	14.35	14.23	11.94	11.44	11.63
σ	0.17	0.14	0.17	0.17	0.14	0.21
Cr <sub>2</sub> O <sub>3</sub>	40.80	33.75	35.19	39.61	39.25	40.00
σ	0.26	0.70	0.23	0.36	0.42	0.52
NiO	b.d.l	b.d.l	b.d.l	0.18	0.18	0.17
σ	-	-	-	0.05	0.08	0.06
ZnO	b.d.l	b.d.l	b.d.l	0.05	0.09	0.08
σ	-	-	-	0.04	0.07	0.06
V <sub>2</sub> O <sub>3</sub>	b.d.l	b.d.l	b.d.l	0.20	0.18	0.18
σ	-	-	-	0.04	0.05	0.03

Table 2 - Representative microprobe analyses of chlorite in the Khoy chromitites.

Samples	SiO <sub>2</sub>	TiO <sub>2</sub>	Al <sub>2</sub> O <sub>3</sub>	FeO	MnO	MgO	CaO	K <sub>2</sub> O	Na <sub>2</sub> O	Cr <sub>2</sub> O <sub>3</sub>	NiO	Total
MM1:												
MM1 1*	28.55	0.01	19.22	1.05	0.00	30.84	0.03	0.02	0.00	2.07	0.41	82.19
MM1 2*	30.57	0.03	15.57	0.94	0.00	33.09	0.07	0.02	0.00	2.37	0.57	83.24
MM1 3*	31.12	0.01	15.39	0.84	0.04	32.35	0.07	0.02	0.01	2.12	0.37	82.32
MM1 4*	28.32	0.02	19.47	0.99	0.03	31.60	0.05	0.01	0.00	2.18	0.53	83.19
MM1 5*	28.80	0.03	19.98	0.97	0.00	32.28	0.02	0.00	0.00	0.88	0.50	83.46
MA2:												
MA2 1*	29.35	0.02	18.69	1.06	0.00	31.09	0.08	0.01	0.00	0.39	0.20	80.90
MA2 2*	28.45	0.01	20.22	1.38	0.00	31.55	0.00	0.01	0.00	1.15	0.13	82.90
MA2 3*	28.54	0.02	20.18	1.01	0.00	30.96	0.00	0.01	0.01	0.31	0.25	81.28
MA2 4*	28.24	0.00	20.97	1.03	0.04	31.60	0.00	0.01	0.00	0.17	0.16	82.22
MA2 5*	28.78	0.01	20.24	1.17	0.00	31.70	0.02	0.00	0.00	0.08	0.17	82.17
MA2 1**	27.90	0.02	21.31	1.31	0.03	31.83	0.01	0.01	0.00	1.45	0.22	84.08
MA2 2**	37.69	0.00	0.50	1.31	0.00	21.19	0.49	0.03	0.03	0.69	0.40	62.32
MA2 3**	39.24	0.00	0.57	1.39	0.01	24.76	0.50	0.02	0.02	0.68	0.44	67.63
MA2 4**	0.62	0.03	0.07	0.35	0.00	21.10	36.92	0.01	0.00	0.30	0.00	59.40
MA2 5**	27.24	0.01	20.45	1.04	0.02	30.65	0.07	0.03	0.01	1.74	0.16	81.41
MA365:												
MA365 1*	27.92	0.02	21.71	1.32	0.04	32.22	0.00	0.00	0.00	0.21	0.28	83.73
MA365 2*	28.25	0.01	21.29	1.25	0.04	31.39	0.09	0.00	0.01	0.57	0.32	83.21
MA365 3*	30.02	0.03	18.54	1.28	0.00	32.68	0.01	0.00	0.01	0.03	0.28	82.87
MA365 4*	27.48	0.01	21.66	1.12	0.03	31.54	0.02	0.00	0.00	0.72	0.35	82.93
MA365 5*	30.99	0.01	16.65	1.08	0.01	33.22	0.04	0.03	0.01	0.24	0.11	82.38
MA365 1**	30.03	0.13	16.90	1.40	0.00	33.34	0.00	0.02	0.00	2.02	0.26	84.10
MA365 2**	27.47	0.00	21.17	1.60	0.07	31.48	0.00	0.01	0.01	1.74	0.25	83.79
MA365 3**	28.02	0.01	20.45	1.69	0.00	31.54	0.04	0.00	0.00	1.87	0.21	83.82
MA365 4**	30.14	0.01	17.32	1.22	0.00	32.86	0.05	0.18	0.00	1.74	0.15	83.68
MA365 5**	27.43	0.00	21.41	1.91	0.06	31.01	0.06	0.03	0.01	1.59	0.23	83.73

\* = in the chromite matrix, \*\* = in contact with chromite.

The PGM were investigated in situ by scanning polished sections under the reflected light microscope at 250-800 magnification and by scanning electron microscopy using a Jeol JXA-8200 instrument. Then they were analyzed using the same instrument in the WDS mode, at 20 kV accelerating voltage and 10 nA beam current, performing a beam diameter of about 1 micron or less. The counting time on peak and backgrounds were 15 and 5 seconds respectively. The  $K\alpha$  lines were used for S, As, Fe, Cu and Ni;  $L\alpha$  for Ir, Ru, Rh and Pt, and  $M\alpha$  for Os. The reference materials were pure metals for the six PGE (Ru, Rh, Pd, Os, Ir, Pt), synthetic NiS, natural chalcopyrite and niccolite for Ni, Fe, Cu, S and As. The following diffracting crystals were selected: PETJ for S, PETH for Ru, Os, Rh, LIF for Cu, LIFH for Ni, Ir, Pt and TAP for As. Automatic corrections were performed for interference involving Ru-Rh, Ir-Cu and Rh-Pd. The detection limits of the analyzed elements, are 1000 ppm for Ir and Pt, 800 for Os, 400 for As, Ni and Cu, 200 for Ru, Pd and Fe, 100 for S and Rh. Selected PGM analyses are presented in Table 3.

Two chromitite samples were analyzed for the six PGE and Au in the laboratory of Genalyses (Australia) by ICP-MS after Ni-sulfide pre-concentration (Table 4).

## RESULTS

### Texture and composition of chromite

Reflected light microscope investigation reveals that only chromitites from MM1 are massive (< 10% interstitial silicate), interrupted by cracks and pull-a-part fractures (Fig.

3A). Chromitites from MA365 and MA2 are characterized by orbicular texture with more than 50% chromite by volume. The texture consists of sub-rounded chromite aggregates up to 3 mm in size, in a matrix mainly composed of altered silicates (Fig. 3B, C). Some chromite grains occur in contact with carbonates (calcite and probably dolomite) and uvarovite (Fig. 3D). In sample MA365 the orbicular texture is partially obliterated by the presence of a strongly brecciated and fractured zone. Samples ATD consist of massive chromitite. Primary chromite, from unaltered grain cores, shows little compositional variation from one locality to the other (Table 1). Chromite is generally Al-rich, however, the massive chromitites from MM1 show a slight enrichment in  $Cr_2O_3$ .

The calculated amount of  $Fe_2O_3$  is lower than 1.8 wt% and the  $TiO_2$  content is less than 0.2 wt%, except in the ATD samples, that contain up to 0.65 wt% of  $TiO_2$ . The chromite compositions plotted in suitable diagrams fall unequivocally in the field of podiform chromitites (Fig. 4A, B, C). They also display a similarity with chromitites crystallized from MORB-type magmas (Fig. 4D). The Khoy chromitites are characterized by different alteration patterns. Samples MA365 and MA2 are characterized by a fresh chromite core (Fig. 5A, B) in outer contact with an irregular zone filled with secondary minerals, such as chlorite, uvarovite and carbonates (Fig. 3D). The more external rim is composed of altered oxides, corresponding to ferrian chromite and minor magnetite. The alteration pattern of sample MM1 consists of a thin rim of ferrian chromite developed on the external border of chromite grains and along cracks.

Table 3 - Representative analyses of laurite in the Khoy chromitites.

Sample	Os	Ir	Pt	Ru	Rh	Pd	Fe	Ni	Cu	S	As	Total
Weight %												
atd11 3 1	12.68	4.36	b.d.l	41.09	1.82	2.44	1.38	0.06	0.10	35.86	0.52	100.30
atd11 3 2	12.86	4.59	b.d.l	41.45	1.86	2.45	1.32	0.05	0.09	36.50	0.52	101.69
atd1 1 1	20.64	7.00	b.d.l	31.59	1.36	1.76	1.55	0.12	0.19	34.13	0.42	96.82
atd1c 2 1	25.94	2.29	b.d.l	32.90	1.29	1.78	1.27	0.06	0.07	34.26	0.39	99.10
atd1c 2 2	25.74	2.31	b.d.l	31.22	1.27	1.74	1.40	b.d.l	0.08	33.09	0.40	97.27
Atomic %												
atd11 3 1	3.95	1.34	b.d.l	24.07	1.05	1.36	1.46	0.06	0.09	66.21	0.41	
atd11 3 2	3.94	1.39	b.d.l	23.93	1.06	1.34	1.38	0.05	0.08	66.42	0.41	
atd1 1 1	6.82	2.29	b.d.l	19.65	0.83	1.04	1.75	0.13	0.19	66.94	0.36	
atd1c 2 1	8.52	0.74	b.d.l	20.33	0.78	1.05	1.41	0.07	0.07	66.71	0.33	
atd1c 2 2	8.74	0.78	b.d.l	19.94	0.79	1.05	1.62	b.d.l	0.08	66.61	0.35	

Table 4 - PGE concentration (ppb) of the Khoy chromitites.

Samples	Os	Ir	Ru	Rh	Pt	Pd	Total PGE
KHYD10	26	31	62	8	30	19	131
KHYD15	27	32	74	6	17	20	129

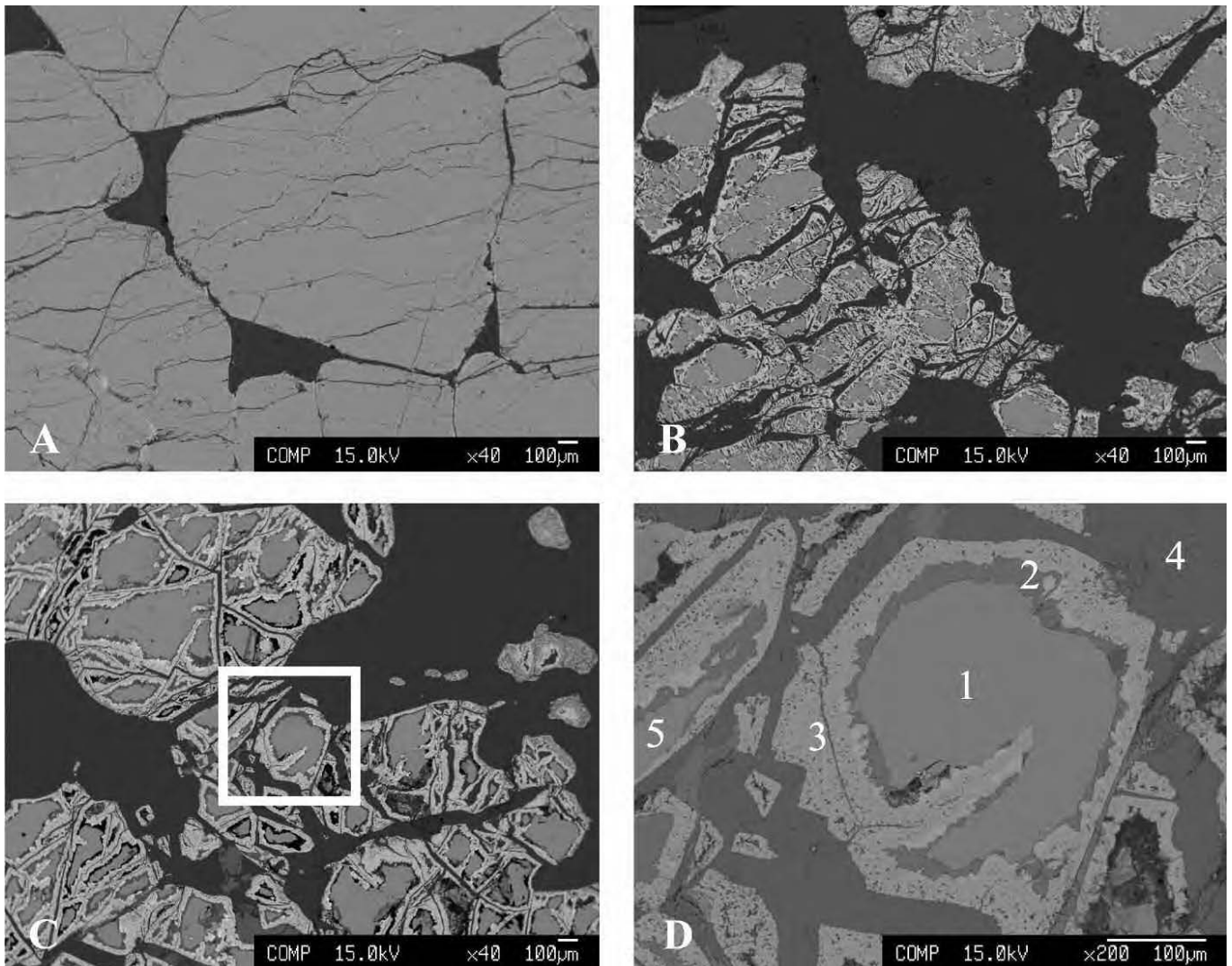


Fig. 3 - Back-scattered-electron (BSE) images showing different textures of the investigated chromitites. A = sample MA365, B = sample MM1, C = sample MA2 and D = enlargement of C image. 1 = chromite, 2 = calcite, 3 = ferrian chromite, 4 = chlorite and 5 = uvarovite.

### Chlorite composition and its geothermometry significance

Two different types of chlorite have been analyzed, one is part of the interstitial silicate matrix, the other occurs in contact with the altered rims of the chromite crystals.

Chlorite geothermometers based on  $^{IV}Al$ -Si reciprocal substitution (Cathelineau and Nieva 1985; Kranidiotis and MacLean 1987; Zang and Fyfe 1995) gave average results in the range of 208-313°C, with chlorite from the interstitial matrix being shifted to the lower thermal range. Our data indicate, as a whole, that the obtained temperatures in chlorite from the matrix are lower than those registered in chlorite found in the alteration rim of the chromite (Table 5). However, we are aware that the possible influence of structurally bound Cr on the equilibria, which these geothermometers are based on, has not been studied experimentally, as previously noticed by Zaccarini et al. (2006).

### PGE and PGM distribution

Whole rocks analyses show that the total PGE concentrations in the Khoy chromitite are very low (129 and 131 ppb) with chondrite-normalised PGE patterns characterized by

high  $(Os + Ir + R)/(Rh + Pt + Pd)$  ratios and consistent positive anomaly in Ru, and negative anomaly in Pt (Fig. 6). In agreement with geochemical data, only PGM containing Os, Ir and Ru as major constituents have been found in the Khoy chromitites. They consist of small grains, variable in size from 1 to 8 microns. Only 12 PGM were found in the ATD and MM1 samples and most of them consist of laurite accompanied by other rare PGM, that due to their small size, have been only qualitatively analyzed. They have been classified as erlichmanite, osmium and unnamed Ir-Cu sulfides (probably cuproiridsite). They form small sub-euhedral grains generally included in fresh chromite (Fig. 7A, B, C). Laurite is the most common PGM, usually occurring as phase crystals (Fig. 7A), and rarely associated with clinopyroxene (Fig. 7B) and other PGM (Fig. 7C). Only one grain of erlichmanite associated with laurite and osmium was found in contact with ferrian chromite (Fig. 7D). The laurite composition has been plotted, as at %, in the ternary diagram of Fig. 8. This diagram shows that the laurite contains few amounts of Os and Ir and its composition is almost constant. The analyzed laurite is characterized by a relatively high concentration of Pd (Table 3), as previously reported from few other chromitites of Troodos (Cyprus), Bulquiza (Alba-

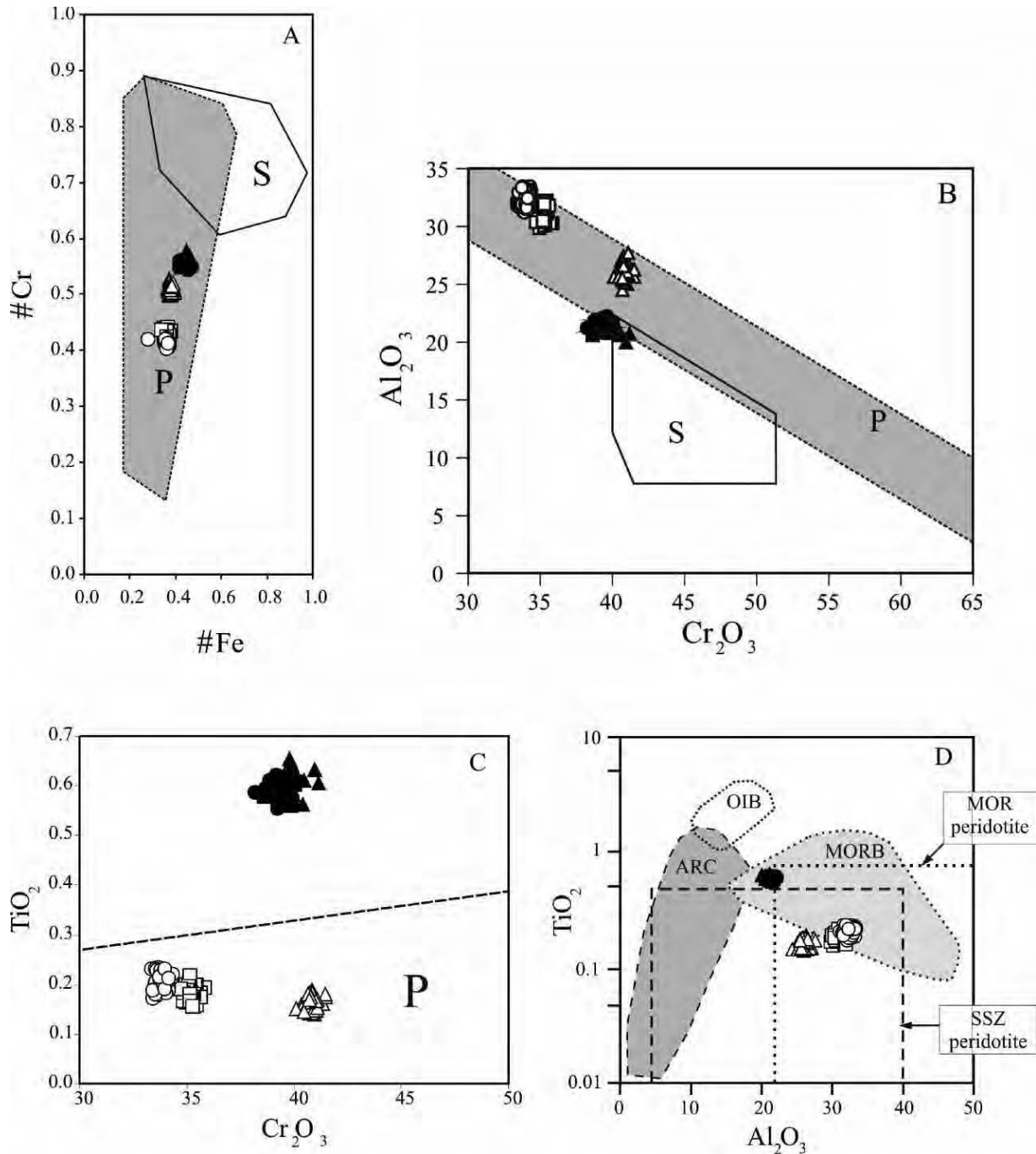


Fig. 4 - Variations of #Cr versus #Fe (A),  $\text{Cr}_2\text{O}_3$  versus  $\text{Al}_2\text{O}_3$  (B), and  $\text{TiO}_2$  as a function of  $\text{Cr}_2\text{O}_3$  and  $\text{Al}_2\text{O}_3$  (C, D) for chromite from the Khoy chromitites. Open square: sample MA365; open circle: sample MA2; open triangle: sample MM1; black square: sample ATD1; black circle: ATD11; black triangle: ATD20. Fields for ocean island basalts (OIB), volcanic arc (ARC), mid-ocean-ridge basalts (MORB), and mantle peridotite in SSZ and MOR settings are after Roeder (1994) and Kamenetsky et al. (2001). P = ophiolitic podiform chromitite, S = stratiform chromitite.

nia), Nurali (Urals) and Santa Elena (Costa Rica) (McElduff and Stumpfi, 1990; Zaccarini et al., 2004; 2011).

## DISCUSSION

### Magmatic significance of the Khoy chromitites and associated PGM

Maurel and Maurel (1982) proposed a theoretical model in which high-Cr or metallurgical chromites crystallize from

Al-poor melts, such as picritic or boninitic basalts, whereas high-Al or refractory chromites precipitate from a N-MORB melt. There is a general agreement that the Cr-rich podiform chromitites form in a SSZ environment, because of the melt-melt or melt-rock interaction, in the presence of fluids (Zhou and Robinson, 1997; Ballhaus, 1998). Al-rich chromitites are generated by decompression melting at seafloor spreading centers in two distinct geodynamic settings: 1) in a back-arc basin of a SSZ, or 2) in the mid ocean ridge. Consistently, Cr-rich chromitites are associated with

Table 5 - Results of chlorite geothermometry.

Samples	No. of analyses	Cathelineau and Nieva, 1985	Hiller and Velde, 1991	Kranidiotis and Maclean, 1987	Zang and Fyfe, 1995
MM1: MM1 *	9	Max=282, Min=252 Mean=270, $\sigma$ = 11.25	Max=279, Min=129, Mean=208, $\sigma$ = 58.56	Max=276, Min=212, Mean=246, $\sigma$ = 24.94	Max=305, Min=241, Mean=275, $\sigma$ = 24.83
MA2: MA2 *	10	Max=276, Min=253, Mean=264, $\sigma$ = 8.40	Max=281, Min=133, Mean=234, $\sigma$ = 42.92	Max=277, Min=214, Mean=257, $\sigma$ = 18.34	Max=305, Min=243, Mean=286, $\sigma$ = 18.13
MA2 **	7	Max=295, Min=257, Mean=280, $\sigma$ = 12.03	Max=335, Min=217, Mean=286, $\sigma$ = 45.81	Max=300, Min=250, Mean=279, $\sigma$ = 19.58	Max=328, Min=278, Mean=308, $\sigma$ = 19.35
MA365: MA365 *	9	Max=290, Min=265, Mean=279, $\sigma$ = 8.27	Max=323, Min=58, Mean=218, $\sigma$ = 88.65	Max=295, Min=182, Mean=250, $\sigma$ = 37.79	Max=323, Min=211, Mean=279, $\sigma$ = 37.55
MA365 **	10	Max=296, Min=283, Mean=289, $\sigma$ = 5.32	Max=337, Min=202, Mean=300, $\sigma$ = 50.72	Max=301, Min=243, Mean=286, $\sigma$ = 21.77	Max=329, Min=272, Mean=313, $\sigma$ = 21.30

\* = in the chromite matrix, \*\* = in contact with chromite.

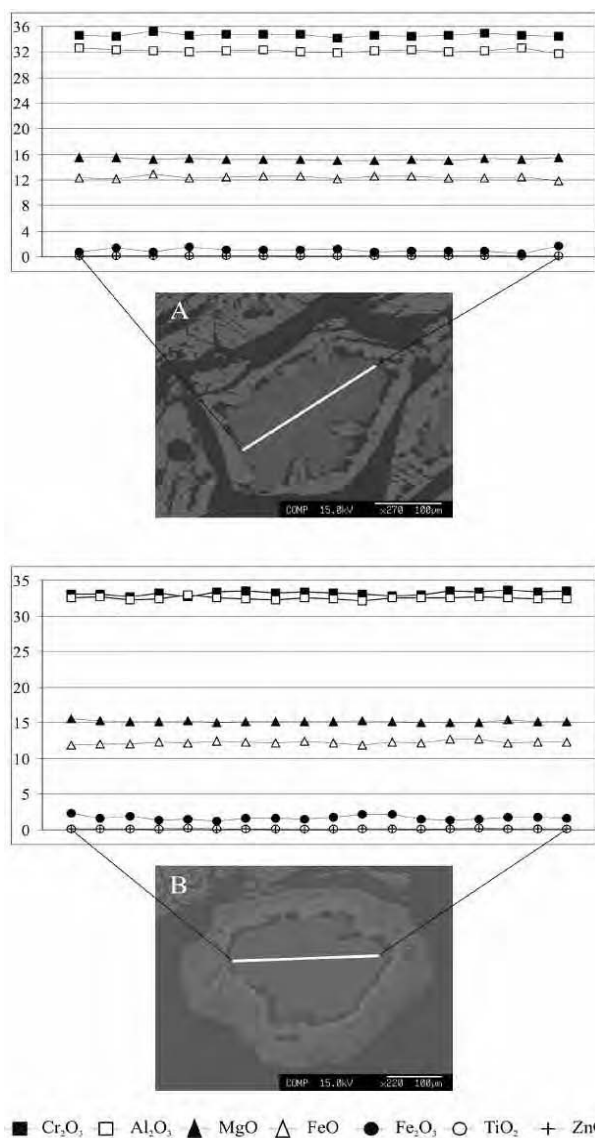


Fig. 5 - Compositional variations of Cr<sub>2</sub>O<sub>3</sub>, Al<sub>2</sub>O<sub>3</sub>, MgO, FeO, Fe<sub>2</sub>O<sub>3</sub>, TiO<sub>2</sub> and ZnO (wt%) through selected altered chromite grains of the Khoys chromitites. A = sample MA365, B = sample MA2.

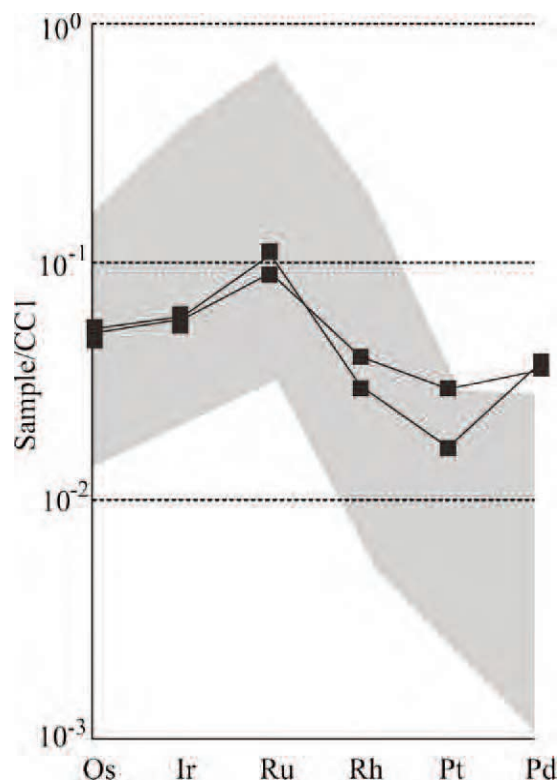


Fig. 6 - Chondrite normalized PGE patterns for chromitite from the Khoys ophiolite. Field (light grey) of mantle-hosted ophiolitic chromitite after Zaccarini et al. (2011) and references therein. CCI normalization values from Naldrett and Duke (1980).

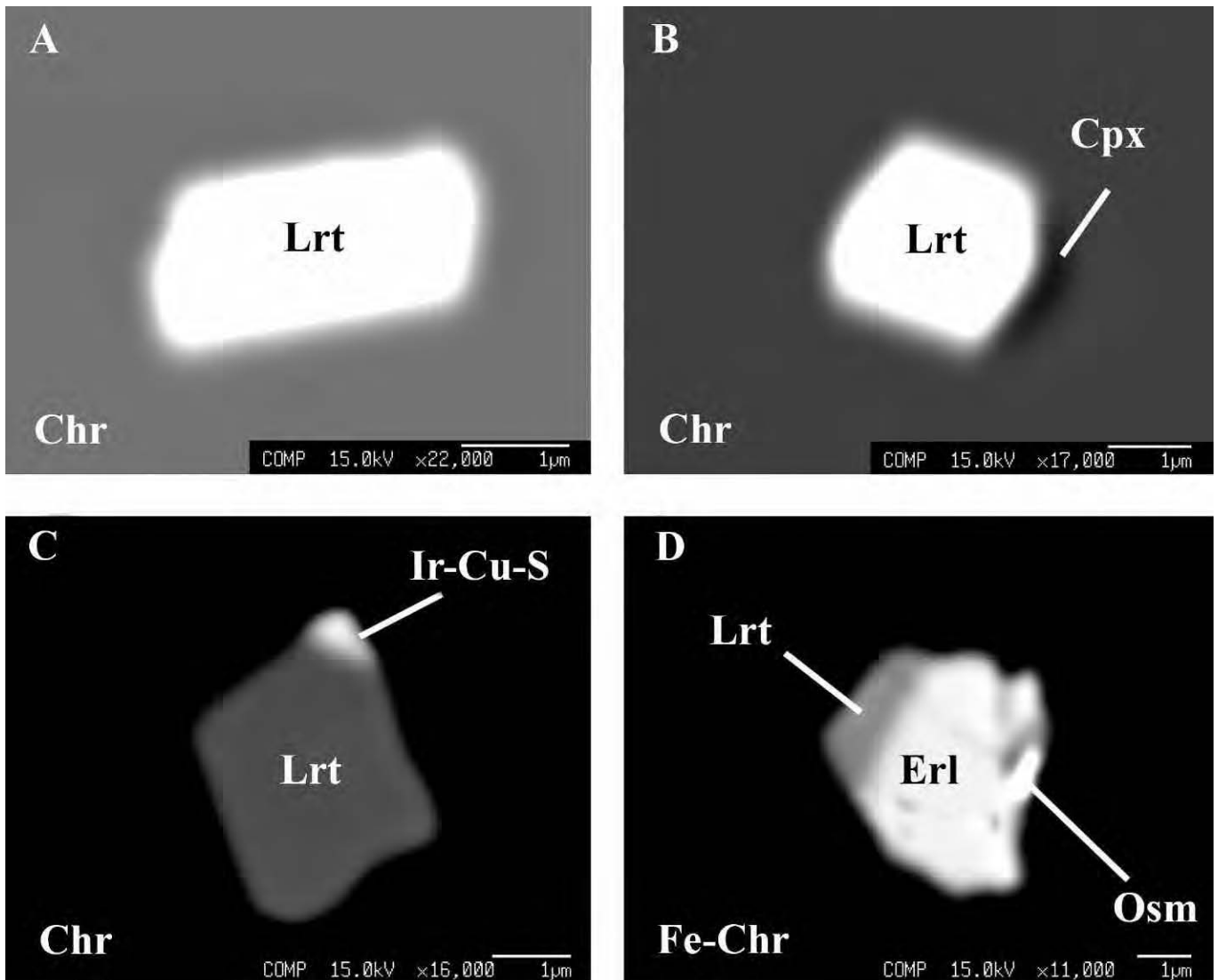


Fig. 7 - Back-scattered-electron (BSE) images of PGM associated with the Khoy chromitites. A = single phase laurite, B = laurite associated with clinopyroxene, C = laurite and unnamed Ir, Cu sulfide, D = composite PGM of erlichmanite, laurite and osmium. PGM in Figs. A, B, C are included in fresh chromite, PGM in Fig. D is in contact with ferrian chromite. Abbreviations: Lrt = laurite, Chr = chromite, Cpx = clinopyroxene, Ir-Cu-S = unnamed Ir, Cu sulfide, Erl = erlichmanite, Osm = osmium, Fe-Chr = ferrian chromite.

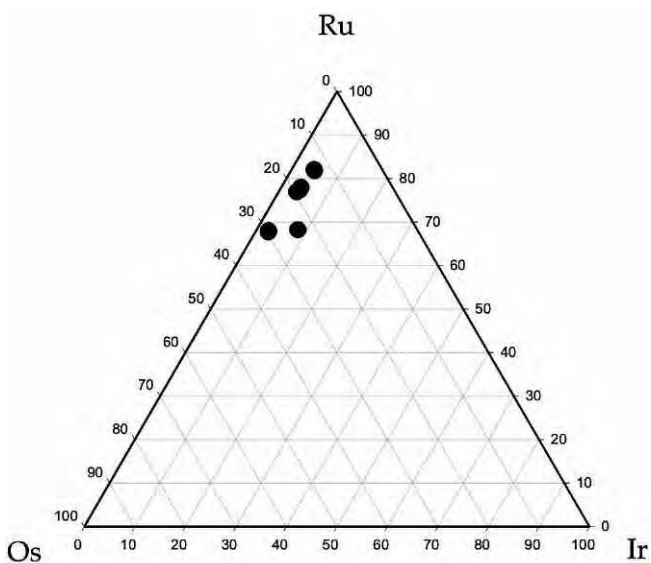


Fig. 8 - Composition (at%) of laurite of the Khoy chromitites in the Os-Ru-Ir ternary system.

harzburgite and dunite, whereas Al-rich chromitites occur with harzburgite and lherzolite (Leblanc and Nicolas, 1992).

Recently, using the equation of Rollinson (2008) and data from Kamenetsky et al. (2001), it has been demonstrated that it is possible to evaluate the melt composition in equilibrium with the crystallizing chromite, only using the chromite composition (see Zaccarini et al., 2011 and references therein). Using this approach, we have estimated the  $\text{Al}_2\text{O}_3$  and  $\text{TiO}_2$  contents of melts in equilibrium with the Khoy chromitites. The calculated data, plotted in Fig. 9 unequivocally indicate that the Khoy chromitites precipitated from a MOR melt suggestive of an extensional geological setting. However, it was not possible to unequivocally establish whether the Al-rich chromitites of Khoy formed in a back arc basin or in a middle ocean ridge. Nevertheless, the absence of Cr-rich chromitite, typical of SSZ, in the Khoy ophiolite, suggests that the mid ocean ridge is a more likely environment of formation for the Khoy Al-rich chromitite and associated peridotite. A similar scenario was also proposed for some Al-rich chromitites hosted in the Turkish ophiolites of Muğla and Kahramanmaraş (Uysal et al., 2007; 2009).

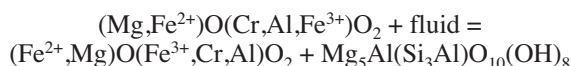
With few exceptions, the Os-Ir-Ru PGM-sulfides display textural relation with the host chromite suggestive of crystallization at high temperature, possibly prior to or concomitant with the crystallization of chromite. According to the model proposed by Tredoux et al. (1995), PGE in natural magmas initially occur as a suspension of clusters of a few hundred atoms in the metallic state. Owing to their specific chemical and physical properties, these clusters tend to coalesce together and adsorb particular ligands (S, As, Te, Bi, Sb) without formal chemical bonding. With decreasing temperature, the clusters start to form specific PGM alloys or compounds with one of the above ligands, characterized by specific crystalline structure. Subsequently, these primary PGM are mechanically entrapped by the early-precipitating minerals, such as chromite and rarely, olivine and pyroxene.

Recent investigations (Brenan and Andrews, 2001; Bockrath et al., 2004; Uysal et al., 2007; El Ghorfi et al., 2008 and references therein) showed that formation of magmatic PGM in podiform chromitites is controlled by the following three main parameters: 1) availability of PGE in the system, 2) temperature, and 3) sulfur fugacity. Sulfur fugacity increases with decreasing temperature and this variation produces effects on the paragenesis and crystallization order of magmatic PGM. Therefore, at very high temperature (around 1300°C) laurite precipitates in equilibrium with Os-Ir-(Ru) alloys. Substitution of Os for Ru in laurite increases with decreasing temperature and increasing sulfur fugacity, therefore the stability field of laurite expands up to reach the composition of erlichmanite. The compositional zoning visible in some laurite grains that generally display Os enrichment in the rim is also indicative of this magmatic evolution. As a consequence, the magmatic composition of minerals of the laurite-erlichmanite series can be used as an efficient tool to model conditions of PGM precipitation, with special regards to temperature and sulfur fugacity.

In the Khoy chromitites, the presence of abundant laurite and the absence of magmatic Os-Ir-(Ru) alloys and erlichmanite suggest that the PGM precipitated in a narrow range of temperature, around 1000°C, at relatively low sulfur fugacity. The absence of hydrous silicates in the primary PGM assemblage of Khoy indicates a fluid-poor environment. This is in contrast with PGM assemblages from SSZ-chromitites in which crystallization of amphibole and other hydrous silicates systematically accompanies precipitation of PGM (Johan et al., 1983; Melcher et al. 1997; Garuti et al., 1999).

#### Alteration of chromite and associated minerals

The first author documenting the alteration product of chromite was Spangeberg (1943) that described ferritchromite as “an opaque substance that, according to chemical and physical properties, must lie between chromite and magnetite”. More recent literature (Beeson and Jackson, 1969; Kimball, 1990) reports that the common hydrothermal alteration of chromite results in increasing  $\text{Cr}_2\text{O}_3$  and  $\text{FeO}$  at the expenses of  $\text{Al}_2\text{O}_3$  and  $\text{MgO}$ , thus confirming the formation of ferritchromite. In the presence of  $\text{SiO}_2$  rich solutions, the Mg and Al released during hydrothermal alteration of magmatic chromite are incorporated in crystallizing chlorite at temperature around 400°C throughout the following chemical reaction:



According to several observations, altered chromite

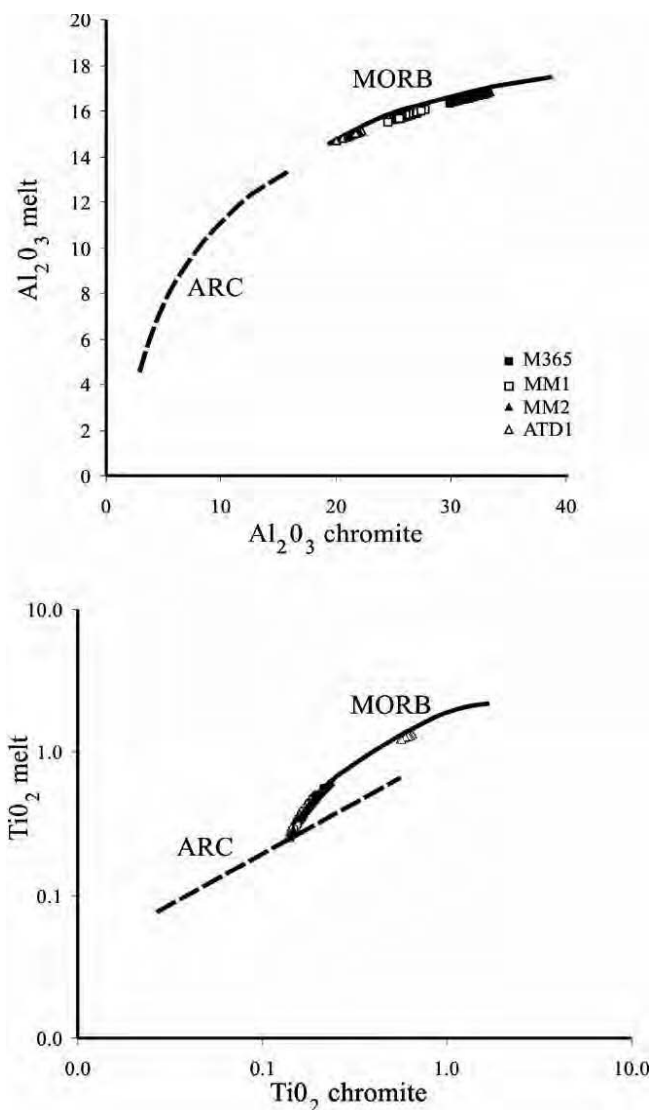


Fig. 9 - Calculated  $\text{Al}_2\text{O}_3$  and  $\text{TiO}_2$  contents in parental melts of chromitite from the Khoy ophiolite. Regression lines for MORB and ARC lavas are based on Kamenetsky et al. (2001) and Zaccarini et al. (2011).

shows a chemical zoning including a fresh core surrounded by one or more rims, with the external one consisting of ferritchromite. Although it is relatively easy to recognize the effects of alteration on the chromite crystals, it is not always possible to establish the precise metamorphic conditions in which the alteration process occurred. Chromite alteration can represent the result of low temperature metamorphism (i.e., ocean floor serpentinization and hydrothermal processes) and it can also be produced under greenschist and amphibolite facies (Ulmer, 1974; Barnes, 2000; Mellini et al., 2005; Proenza et al., 2004; Garuti et al., 2007, among others). According to Barnes (2000), spinels metamorphosed under greenschist facies conditions have  $\text{Mg}/(\text{Mg} + \text{Fe}^{2+})$  values comprised between 0.4 and 0.7, whereas the  $\text{Mg}/(\text{Mg} + \text{Fe}^{2+})$  values in spinels modified under amphibolite facies metamorphism are lower than 0.35. The average  $\text{Mg}/(\text{Mg} + \text{Fe}^{2+})$  value of the altered chromites rims of the Khoy chromitites is 0.56. Therefore, it is not consistent with values typical of amphibolite facies metamorphism. The presence of abundant Ca-bearing secondary minerals, such as calcite and uvarovite, associated with the Khoy chromitite,

suggests that they formed by leaching of Ca from magmatic minerals, probably clinopyroxene. Proenza et al. (1999) reported the presence of secondary uvarovite in the chromitites of Moa Baracoa, Cuba. The Cuban uvarovite formed during low temperature processes related with the formation of chlorite and altered chromite (Proenza et al., 1999). The same scenario was proposed for uvarovite described in the podiform chromitite of Rutland ophiolite (India) (Ghosh and Morishita, 2011). A similar origin can be postulated for uvarovite of the Khoy chromitites. This assumption is also supported by the calculated temperature of chlorite formation that is, with few exceptions, comprised between 300 and 150°C.

## SUMMARY AND CONCLUSIONS

1) According to their magmatic composition, the podiform chromitites of the Khoy ophiolite can be classified as Al-rich. This suggests that they did not precipitate from a boninitic melt related to a SSZ, in a compressive geodynamic setting. More likely, they crystallized from a normal MORB type melt in an extensional regime. This observation is consistent with the model proposed by several authors (McCall and Kidd, 1982; Şengör, 1990; McCall, 1997; Hassinapak and Ghazi, 2000; Khalatbari et al., 2006) that consider a portion of the Khoy massif as an ophiolite formed at a slow-spreading center in a narrow ocean. The similarity between the Khoy chromitites and some Turkish ophiolitic chromitites (Kahramanmara and Muğla; Uysal et al., 2007 and 2009) suggests a possible genetic link, in agreement with the idea that the Khoy ophiolite was part of a narrow Mesozoic ocean that once surrounded the Central Iran Microcontinent and connected western Makran with northwestern Iran and eastern Turkey (McCall and Kidd, 1982; Şengör, 1990; McCall, 1997).

2) Although we cannot exclude that the Khoy chromitites were affected by metamorphism in amphibolite facies, the mineralogical data presented in this contribution suggest that, more likely, they were altered during ocean floor metamorphism. This observation is in agreement with the idea of Pessagno et al. (2005), implying that there is no genetic link between the Early Cretaceous amphibolite block and the Late Jurassic ultramafic rocks containing the investigated Khoy chromitites, although they occur in the same area.

3) Our mineralogical observations suggest that most of the Khoy PGM are magmatic in origin and were not affected by important alteration processes. They crystallized in a narrow range of temperature, around 1000°C, at relatively low sulfur fugacity and in the absence of fluids. This observation is also consistent with the fact that the Khoy chromitites are not related to a SSZ.

## ACKNOWLEDGMENTS

We thank the University Centrum for Applied Geosciences (UCAG) for allowing access to the E. F. Stumpfl electron microprobe laboratory. We are grateful to Riccardo Tribuzio and to an anonymous referee for their useful and constructive comments. Many thanks are also due to Luca Pandolfi and Valerio Bortolotti for their editorial handling. Benedetta Treves improved the English of the manuscript. Her help is greatly appreciated.

## REFERENCES

- Alavi M., 1991. Tectonic map of the Middle East, Scale 1:5.000.000. Geol. Survey Iran, 1 sheet.
- Alavi M., Vaziri H., Seyed-Hemami K. and Lasemi Y., 1997. Triassic and associated rocks of the Nakhlak and Aghdarband areas in central and northeastern Iran as remnants of the southern Turanian active continental margin. *Geol. Soc. Am. Bull.*, 109: 1563-1575.
- Azizi H., Moinevaziri H., Mohajjel M. and Yagobpoor A., 2006. PT path in metamorphic rocks of the Khoy region (northwest Iran) and their tectonic significance for Cretaceous-Tertiary continental collision. *J. Asian Earth Sci.*, 27: 1-9.
- Ballhaus C., 1998. Origin of podiform chromite deposits by magma mingling. *Earth Planet. Sci. Lett.*, 156: 185-193.
- Barnes S.J., 2000. Chromite in komatiite, II. Modification during greenschist to mid-amphibolite facies metamorphism. *J. Petrol.*, 41: 387-409.
- Barnes S.J. and Roeder L.P., 2001. The range of spinel compositions in terrestrial mafic and ultramafic rocks. *J. Petrol.*, 42: 2279-2302.
- Beeson M.H. and Jackson E.J., 1969. Chemical composition of altered chromites from the Stillwater Complex, Montana. *Am. Mineral.*, 54: 1084-1100.
- Bockrath C., Ballhaus C. and Holzheid A., 2004. Stabilities of laurite RuS and monosulfide liquid solution at magmatic temperature. *Chem. Geol.*, 208: 265-271.
- Brenan J.M. and Andrews D.R.A., 2001. High-temperature stability of laurite and Ru-Os-Ir alloys and their role in PGE fractionation in mafic magmas. *Can. Mineral.*, 39: 341-360.
- Cathelineau M. and Nieva D., 1985. A chlorite solid solution geothermometer. The Los Azufres (Mexico) geothermal system. *Contrib. Mineral. Petrol.* 91: 235-244.
- Dick H.J.B. and Bullen T., 1984. Chromian spinel as a petrogenetic indicator in abyssal and alpine-type peridotites and spatially associated lavas. *Contr. Mineral. Petrol.*, 86: 54-76.
- El Ghorfi M., Melcher F., Oberthur T., Boukhari A.E., Maacha L., Maddi A. and Mhaili M., 2008. Platinum group minerals in podiform chromitites of Bou Azzer ophiolite, Anti Atlas, Central Morocco. *Mineral. Petrol.*, 92: 59-80.
- Garuti G., Proenza J.A. and Zaccarini F., 2007. Distribution and mineralogy of platinum-group elements in altered chromitites of the Campo Formoso layered intrusion (Bahia State, Brazil): control by magmatic and hydrothermal processes. *Mineral. Petrol.*, 89: 159-188.
- Garuti G., Zaccarini F., Moloshag V. and Alimov V., 1999. Platinum-group minerals as indicators of sulfur fugacity in ophiolitic upper mantle: an example from chromitites of the Rai-Iz ultramafic complex, Polar Urals, Russia. *Can. Mineral.*, 37: 1099-1115.
- Ghazi A.M., Pessagno E.A., Hassinapak A.A., Kariminia S.M., Duncan R.A. and Babaie H.A., 2003. Biostratigraphic zonation and  $^{40}\text{Ar}/^{39}\text{Ar}$  ages for the Neotethyan Khoy ophiolite of NW Iran. *Palaeo. Palaeo. Palaeo.*, 193: 311-323.
- Ghorashi M. and Arshadi S., 1978. Geological map of Khoy quadrangle, scale 1:250.000. Geol. Survey Iran, 1 sheet.
- Ghosh B. and Morishita T., 2011. Andradite-uvarovite solid solution from hydrothermally altered podiform chromitite, rutland ophiolite, Andaman, India. *Can. Mineral.*, 49: 573-580.
- Hassinapak A.A. and Ghazi A.M., 2000. Petrology, geochemistry and tectonic setting of the Khoy ophiolite, northwest Iran: implications for Tehyan tectonics. *J. Asian Earth Sci.*, 18: 109-121.
- Hoeck V., Tomek C., Robertson A. and Koller F., 2002. Preface to Europrobe-Pancardi Symposium "Eastern Mediterranean ophiolites: magmatic processes and geodynamic implications". *Lithos*, 65: ix-xiii.
- Irvine T.N., 1965. Chromian spinel as a petrogenetic indicator. Part I. Theory. *Can. J. Earth Sci.*, 2: 648-672.
- Irvine T.N., 1967. Chromian spinel as a petrogenetic indicator. Part II. Petrological Application. *Can. J. Earth Sci.*, 4: 71-103.

- Johan Z., Dunlop H., LeBel L., Robert J.L. and Volfinger M., 1983: Origin of chromite deposits in ophiolitic complexes: evidence for a volatile- and sodium-rich reducing fluid phase. *Fortschr. Mineral.* 61: 105-107.
- Kamenetsky V.S., Crawford A.J. and Meffre S., 2001. Factors controlling chemistry of magmatic spinel: an empirical study of associated olivine, Cr-spinel and melt inclusions from primitive Rocks. *J. Petrol.*, 42: 655-671.
- Khalatbari-Jafari M., Juteau T., Bellon H. and Emami H., 2003. Discovery of two ophiolite complexes of different ages in the Khoy area (NW Iran). *C.R. Geosci.*, 335: 917-929.
- Khalatbari-Jafari M., Juteau T., Bellon H., Whitechurch H., Cotten J. and Emami H., 2004. New geological, geochronological and geochemical investigations on the Khoy ophiolites and related formations, NW Iran. *J. Asian Earth Sci.*, 23: 507-535.
- Khalatbari-Jafari M., Juteau T. and Cotten J., 2006. Petrological and geochemical study of the Late Cretaceous ophiolite of Khoy (NW Iran), and related geological formations. *J. Asian Earth Sci.*, 27: 465-502.
- Kimball K.L., 1990. Effects of hydrothermal alteration on the composition of chromian spinels. *Contrib. Mineral. Petrol.*, 105: 337-346.
- Kranidiotis P. and MacLean W.H., 1987. Systematics of chlorite alteration at the Phelps Dodge massive sulfide deposit, Matagami, Quebec. *Econ. Geol.*, 82: 1898-1911.
- Leblanc M. and Nicolas A., 1992. Ophiolitic chromitites. *Intern. Geol. Rev.*, 34 (7): 653-686.
- Malekghasemi F. and Somarin A.K., 2005. Petrology and origin of chromite mineralisation in the Khoy area. *Berg Hüttenmänn. Monatsh.*, 10: 358-366.
- Maurel C. and Maurel P., 1982. Étude expérimentale de la distribution de l'aluminium entre bain silicate basique et spinel chromifère. Implications pétrogenétiques: tenore en chrome des spinelles. *Bull. Mineral.*, 10: 197-202.
- McCall G.J.H. and Kidd R.G.W., 1982. The Makran southeastern Iran: the anatomy of a convergent margin active from Cretaceous to present. In: J.K. Leggett (Ed.), *Trench-forearc geology: Sedimentation and tectonics of modern and ancient plate margins*. *Geol. Soc. London Spec. Publ.*, 10: 387-397.
- McCall G.J.H., 1997. The geotectonic history of the Makran and adjacent areas of southern Iran. *J. Asian Earth Sci.*, 15: 517-531.
- McElduff B. and Stumpfl E.F., 1990. Platinum-group minerals from the Troodos ophiolite complex, Cyprus. *Mineral. Petrol.*, 42: 211-232.
- Melcher F., Grum W., Simon G., Thalhammer T.V. and Stumpfl E.F., 1997. Petrogenesis of the ophiolitic giant chromite deposits of Kempirsai, Kazakhstan: a study of solid and fluid inclusions in chromite. *J. Petrol.*, 38 (10): 1419-1458.
- Mellini M., Rumori C. and Viti C., 2005. Hydrothermally reset magmatic spinels in retrograde serpentinites, formation of ferri-chromite rims and chlorite aureoles. *Contrib. Mineral. Petrol.*, 149: 266-275.
- Monsef I.M., Rahgoshay M., Mohajjel M. and Shafaii Moghadam H., 2010. Peridotites from the Khoy Ophiolitic Complex, NW Iran: Evidence of mantle dynamics in a supra-subduction-zone context. *J. Asian Earth Sci.*, 38: 105-120.
- Naldrett A.J. and Duke J.M., 1980. Pt metals in magmatic sulfide ores. *Science*, 208: 1417-1424.
- Pessagno E.A., Ghazi A.M., Kariminia M., Duncan R.A. and Hasinapak A.A., 2005. Tectonostratigraphy of the Khoy Complex, northwestern Iran. *Stratigraphy*, 2: 49-63.
- Proenza J.A., Ortega-Gutierrez F., Camprubi A., Tritlla J., Elias-Herrera M. and Reyes Salas M., 2004. Paleozoic serpentinite-enclosed chromitites from Tehuiztingo (Acatlan Complex, southern Mexico): a petrological and mineralogical study. *J. South Am. Earth Sci.*, 16: 649-666.
- Proenza J.A., Sole J. and Melgarejo J.C., 1999. Uvarovite in podiform chromitite: the Moa-Baracoa ophiolitic massif, Cuba. *Can. Mineral.*, 37: 679-690.
- Robertson A.H.F., 2002. Overview of the genesis and emplacement of Mesozoic ophiolites in the Eastern Mediterranean Tethyan region. *Lithos*, 65: 1-67.
- Roeder P.L., 1994. Chromite: from the fiery rain of chondrules to the Kilauea Iki lava lake. *Can. Mineral.*, 32: 729-746.
- Rollinson H., 2008. The geochemistry of mantle chromitites from the northern part of the Oman ophiolite: inferred parental melt composition. *Contrib. Mineral. Petrol.*, 156: 273-288.
- Şengör A.M.C., 1990. A new model for the late Paleozoic-Mesozoic tectonic evolution of Iran and implications for Oman. In: A.H.F. Robertson, M.P. Searle and A.C. Ries (Eds.), *The geology and tectonics of the Oman Region*. *Geol. Soc. London Spec. Publ.*, 49: 797-831.
- Spangenberg K., 1943. Die Chromitlagerstätte von Tampadel am Zobten. *Z. Prakt. Geol.*, 5: 13-35.
- Stowe C.W., 1994. Compositions and tectonic settings of chromite deposits through time. *Econ. Geol.*, 89: 528-546.
- Thayer T.P., 1970. Chromite segregations as petrogenetic indicators. In: "Symposium on the Bushveld igneous complex and other Layered intrusions". *Geol. Soc. South Africa, Spec. Publ.*, 1: 380-390.
- Tredoux M., Lindsay N.M., Davies G. and McDonald I., 1995. The fractionation of platinum group elements in magmatic system, with the suggestion of a novel causal mechanism. *South Afr. J. Geol.*, 98: 157-167.
- Ulmer G.C., 1974. Alteration of chromite during serpentinization in the Pennsylvania-Maryland district. *Am. Mineral.*, 59: 1236-1241.
- Uysal I., Tarkian M., Sadiklar M.B., Zaccarini F., Meisel T., Garuti G. and Heidrich, S., 2009. Petrology of Al- and Cr-rich ophiolitic chromitites from the Muğla, SW Turkey: implications from composition of chromite, solid inclusions of platinum-group mineral, silicate, and base-metal mineral, and Os-isotope geochemistry. *Contrib. Mineral. Petrol.*, 158: 659-674.
- Uysal I., Zaccarini F., Garuti G., Meisel T., Tarkian M., Bernhardt H.J. and Sadiklar M.B., 2007. Ophiolitic chromitites from the Kahramanmaraş area, southeastern Turkey: their platinum group elements (PGE) geochemistry, mineralogy and Os-isotope signature. *Ophioliti*, 32: 151-161.
- Yaghubpur A. and Hassannejad A.A., 2006. The spatial distribution of some chromite deposits in Iran, using Fry analyses. *J. Sci. Islam. Rep. Iran*, 17: 147-152.
- Zaccarini F., Garuti G. and Martin R.F., 2006. Exotic accessory minerals in layered chromitites of the Campo Formoso complex, Brazil. *Geol. Acta*, 4: 461-469.
- Zaccarini F., Garuti G., Proenza J.A., Campos L., Thalhammer O.A.R., Aiglsperger T. and Lewis J., 2011. Chromite and platinum-group-elements mineralization in the Santa Elena ophiolitic ultramafic nappe (Costa Rica): geodynamic implications. *Geol. Acta*, 9: 407-423.
- Zaccarini F., Pushkarev E., Fershatater G. and Garuti G., 2004. Composition and mineralogy of PGE-rich chromitites in the Nurali lherzolite-gabbro complex, southern Urals. *Can. Mineral.*, 42: 545-562.
- Zang W. and Fyfe W.S., 1995. Chloritization of the hydrothermally altered bedrocks at the Igarape Bahia gold deposit, Carajas, Brazil. *Mineral. Deposita*, 30: 30-38.
- Zhou, M.-F. and Robinson P.T., 1997. Origin and tectonic environment of podiform chromite deposits. *Econ. Geol.*, 92: 259-262.